Environ. Sci. Technol. **1996**, *30,* 2078−2083

Chlorine Penetration into Artificial Biofilm Is Limited by a Reaction−Diffusion Interaction

XIAO CHEN AND PHILIP S. STEWART*

Center for Biofilm Engineering and Department of Chemical Engineering, Montana State University, Bozeman, Montana 59717

The retarded penetration of chlorine into artificial biofilms of *Pseudomonas aeruginosa* entrapped in agarose gel slabs was investigated experimentally and shown to be consistent with an unsteady reaction−diffusion model. A chlorine microelectrode was used to measure transient chlorine concentration profiles in artificial biofilms in a flow cell. While chlorine penetrated relatively quickly into pure agarose films (∼15 min), its penetration into biofilms was greatly retarded when cells were present. The degree of retardation was proportional to the initial cell density in the biofilm. After 3 h of treatment with a flowing chlorine solution, the chlorine concentration at the substratum under a 526 μm thick biofilm containing 14 400 mg L^{-1} cell mass had only risen to 10% of the bulk solution value. A mathematical model of the transient reaction−diffusion interaction correctly captured the qualitative behavior of experimentally measured chlorine concentration profiles. Parameter values for the simulations were obtained from the literature and from independent investigations of biomass−chlorine reactions using well-mixed suspensions. Kinetic and stoichiometric coefficients for the reactions of agarose and cell mass with chlorine were obtained by fitting a simple first-order (in both reactants) kinetic model to chlorine versus time data. The reaction rate coefficient for chlorine−cell reaction (1.1×10^{-3} L mg^{-1} s^{-1}) exceeded that of chlorine−agarose reaction (3.7×10^{-6} L mg^{-1} s^{-1}) by 2 orders of magnitude. The yield coefficient relating the amount of cell mass consumed to the amount of chlorine consumed ranged from 0.6 to 4.3 mg mg^{-1}, depending on the duration of the experiment. This study shows that the reaction rate of chlorine with cellular biomass is fast enough that diffusion of this disinfectant into the biofilm readily becomes rate limiting. This reaction−diffusion interaction affords an excellent explanation for the poor efficacy of chlorine when used against biofilm microorganisms.

* Corresponding author, telephone: (406) 994-2890; fax: (406) 994-6098.

Introduction

This paper addresses the control, using chlorine, of detrimental microbial biofilms that form on wetted surfaces in engineered systems. Biofilm formation in these systems can impede heat and momentum transfer, induce corrosion, and present health risks. Biocides, such as chlorine, are commonly employed to deal with these problems. For example, chlorine is routinely applied to manage biofouling in drinking water distribution networks, industrial cooling water systems, swimming pools, paper mills, food processing equipment, and numerous other systems. Efficient control of biofouling problems is frustrated by the profoundly reduced susceptibility of attached or biofilm microorganisms to disinfectants when compared to their planktonic counterparts (*1*−*3*). The reduced efficacy of chlorine against biofilms becomes a more acute limitation as environmental regulations on the release of chlorine and chlorinated organics grow increasingly stringent (*4*, *5*).

The phenomenological basis for biofilm resistance to chlorine is not well understood, though it has long been suspected that this agent fails to fully penetrate biofilm (*6*). We have recently demonstrated this penetration failure directly by measurements made using a chlorine-sensitive microelectrode (*7*). The purpose of the work reported in this paper was to further elucidate the underlying physical−chemical basis of the retarded penetration of chlorine into biofilm. We hypothesized that a reaction−diffusion interaction was responsible. In other words, chlorine is neutralized by reaction with organic constituents of the biofilm faster than it diffuses into the film. This paper describes an experimental test of this mechanism made in a well-defined artificial biofilm system.

Materials and Methods

Artificial biofilms consisting of bacteria dispersed in agarose gel slabs were used as a model system for the investigation of simultaneous transport and reaction of chlorine. An artificial biofilm system was chosen because it affords a simple geometry, control over such parameters as biofilm thickness and cell density, and good reproducibility. *Pseudomonas aeruginosa* ERC1 was used in pure culture throughout. This environmental isolate and known biofilm former was grown in a rich medium at 27.5 ± 0.5 °C and harvested by centrifugation. Artificial biofilms were prepared by spreading an agarose−cell mixture in a thin layer on a stainless steel slide and allowing the mixture to gel. Agarose solution was prepared by melting 2% agarose (low gelling temperature, type VII, Sigma) in a 65 °C water bath for 30 min. The solution was cooled to about 40 °C and then mixed with an equal volume of washed, resuspended cells to obtain a final gel concentration of 1%. Artificial biofilm thickness was determined optically by the method of Bakke and Olsson (*8*). Each reported thickness represents the average of two measurements at the beginning of the experiment and two at the end of the experiment. The initial cell density and biofilm thickness were varied as summarized in Table 1.

Chlorine concentrations were measured by either an amperometric chlorine microelectrode or by the DPD (*N*,*N*-diethyl-*p*-phenylenediamine) colorimetric method. These measurements were calibrated to a standard chlorine

 S0013-936X(95)00918-7 CCC: $12.00

TABLE 1

Summary of Artificial Biofilm Experimental Conditions[a]

expt	X_{1o} (mg L^{-1})	C_o (mg L^{-1})	L_f (μm)	figure
1	0	10.4	773	4A
2	901	9.8	428	4B
3	983	14.9	476	
4	1 160	13.4	771	
5	4 270	14.2	456	
6	14 400	18.6	526	

[a] The parameters are X_{1o}, initial biomass concentration; C_o, initial chlorine concentration; L_f, biofilm thickness.

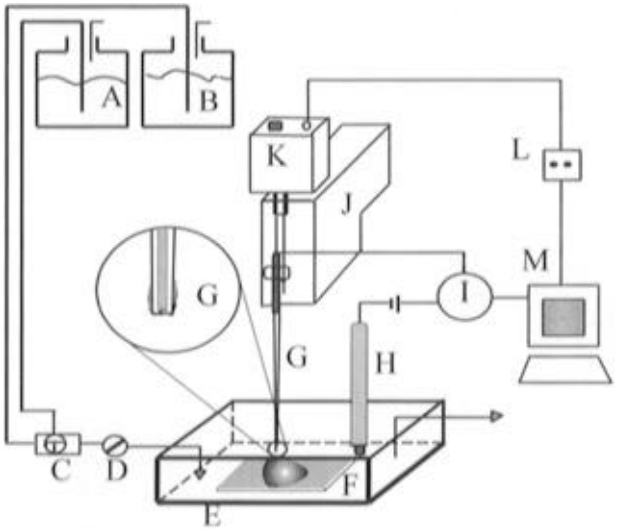

FIGURE 1. Apparatus for chlorine concentration profile measurement within artificial biofilms. Components of the system include A, chlorine solution carboy; B, phosphate buffer carboy; C, three-way valve; D, flow rate control valve; E, flow cell; F, stainless steel slide with artificial biofilm; G, chlorine microelectrode; H, reference electrode; I, picoammeter; J, micromanipulator; K, step motor; L, step motor controller; M, computer for data acquisition and step motor automation.

solution whose concentration was determined by the DPD ferrous titrametric method (*9*). The standard solution concentration was the average of three titration values, whose relative errors between any two values were less than 1%. The chlorine microelectrode consisted of a glass-covered platinum wire with a cellulose acetate coating over the tip, the construction and operation of which has been described elsewhere (*7*). The electrode operated with an applied potential of +0.2 V relative to a saturated calomel electrode. The current through the circuit, which was measured with a picoammeter (Keithley Instruments, Model 480), was directly proportional to the chlorine concentration.

The intrinsic kinetics of chlorine reaction with planktonic biomass were investigated in stirred batch experiments. After mixing a chlorine solution and cell suspension (or agarose solution), the decay of chlorine concentration with time was measured. In short duration experiments (20 min), chlorine concentration was measured using a microelectrode. In a few long-duration experiments (20−24 h), chlorine concentration was measured by the DPD colorimetric method.

Chlorine concentration profiles were measured in artificial biofilms placed in a flow cell (Figure 1). Two carboys supplied the influent by gravity feed. One contained a phosphate buffer solution (4.59 mM, pH 7.2), and the other contained a chlorine solution made by diluting sodium hypochlorite solution in the same buffer. The influent chlorine concentration in each experiment is given in Table 1. Effluent from the flow cell was removed by aspiration. The working volume in the flow cell was approximately 40 mL. Flow rates through the reactor of approximately 400 mL min^{-1} were used corresponding to a hydraulic residence time of 6 s. The chlorine microelectrode was positioned with a micromanipulator coupled to a computer-controlled step motor. A horizontally oriented binocular microscope (7−15×) was used to determine when the microelectrode had reached the surface of the artificial biofilm. Chlorine concentration profiles with depth in the biofilm were determined with a step size of 15−25 μm; 3−5 min was typically required to acquire a single profile.

Mathematical Modeling and Data Analysis

A simple two-constituent reaction model was used to simulate the kinetics of chlorine−biomass reaction. The reaction rate was assumed to be first order with respect to both chlorine and biomass (cells or agarose) concentrations, leading to the following differential balances for the batch system:

$$\frac{dC}{dt} = -kXC \tag{1}$$

$$\frac{dX}{dt} = -kYXC \tag{2}$$

Here C is the chlorine concentration, X is the concentration of chlorine-reactive sites in cells (X_1) or agarose (X_2), k is the reaction rate coefficient, Y is a yield coefficient, and t is time. The concentration of chlorine-reactive sites in biomass is given in terms of equivalents of fresh biomass. That is, initially the concentration of chlorine reactive sites is numerically equal to the dry mass concentration of total biomass. Chlorine reactive sites (but not necessarily total biomass as dry weight) are depleted during exposure to chlorine. The yield coefficient, Y, is the mass of cells or agarose in which reactive sites have been depleted per mass of chlorine consumed. The solution to this system of equations is

$$C = \frac{X_o - YC_o}{-Y + \exp\left[\ln\frac{X_o}{C_o} + (X_o - YC_o)kt\right]} \tag{3}$$

$$X = X_o - Y(C_o - C) \tag{4}$$

where C_o and X_o are the initial values of C and X, respectively.

A nonlinear least-squares method was used to determine values of the two parameters Y and k for each experimental data set. The Marquardt−Levenberg algorithm in the software SigmaPlot (Jandel Scientific) was used.

The penetration of chlorine into an artificial biofilm is amenable to description by reaction−diffusion theory. We assumed that diffusion is the only mass transport mechanism in the film and that the density and effective diffusion coefficient were homogeneous in space. The one-dimensional differential balance on chlorine is

$$\frac{\partial C}{\partial t} = D_e \frac{\partial^2 C}{\partial z^2} - k_1 X_1 C - k_2 X_2 C \quad (5)$$

The four terms in eq 5 represent, from left to right, accumulation, diffusion, reaction with cell mass, and reaction with agarose. D_e denotes the effective diffusion coefficient of chlorine in the biofilm, and z denotes a spatial coordinate normal to the substratum. A no-flux condition at the substratum and a matching-flux condition at the biofilm−bulk fluid interface constitute the boundary conditions for the chlorine balance equation:

$$\frac{\partial C}{\partial t} = 0 \qquad \text{at } z = 0 \qquad \text{for all } t \geq 0 \quad (6)$$

$$D_e \frac{\partial C}{\partial z} = \frac{D_{aq}}{\delta}(C_o - C) \qquad \text{at } z = L_f \qquad \text{for all } t \geq 0 \quad (7)$$

The parameter δ in eq 7 is the dimension of an external mass transfer resistance layer, which is sometimes conceptualized as a stagnant fluid film adjacent to the biofilm. L_f denotes the biofilm thickness.

Neglecting cell growth and detachment, balances on cell mass and agarose are respectively

$$\frac{\partial X_1}{\partial t} = -Y_1 k_1 X_1 C \quad (8)$$

and

$$\frac{\partial X_2}{\partial t} = -Y_2 k_2 X_2 C \quad (9)$$

Once again, the parameters Y_1 and Y_2 in eqs 8 and 9 are yield coefficients that represent the mass of cells (Y_1) or agarose (Y_2) in which chlorine reactive sites are depleted per mass of chlorine consumed. Initial conditions for the biomass balances imposing uniform initial concentrations of both biomass constituents are

$$X_1 = X_{1o} \qquad X_2 = X_{2o} \qquad \text{at } t = 0 \qquad \text{for } 0 \leq z \leq L_f \quad (10)$$

Equations 5−10 were solved using a Gear algorithm implemented in a shared software called XTC.

Results

Most of the chlorine measurements made in this investigation relied on a chlorine microelectrode. This electrode was characterized with respect to its sensitivity to stirring, pH, buffer concentration, interference by oxygen, and applied potential. The microelectrode was not stirring sensitive, exhibiting less than 5% change in signal as the rotation rate of a magnetic stir bar in the sensed solution was varied from 0 to 1000 rpm. It was sensitive to pH, in a manner similar to that reported previously (*7*). Because all of the solutions used were well buffered, pH changes were negligible. The electrode signal was independent of buffer concentration between about 50 and 200% of the buffer concentration used in experiments. Below approximately 50% buffer concentration, the electrode signal declined sharply. Oxygen contributed to the electrode signal at applied potentials less than approximately 0.0 V as determined by alternatively purging the measurement solution with air or with nitrogen. At the applied potential used for chlorine measurement in this study, +0.2 V, air-sparged and nitrogen-sparged signals were identical. In addition to precluding interference by oxygen, the applied potential of +0.2 V provided an optimal signal to background ratio (Figure 2).

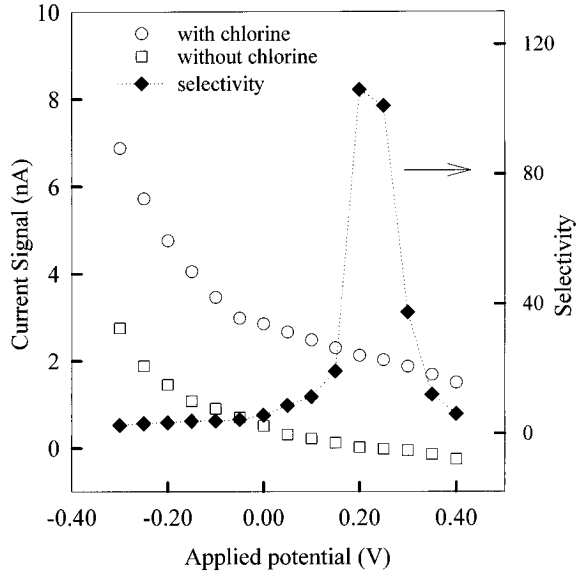

FIGURE 2. Sensitivity and selectivity of chlorine microelectrode at different applied potentials. Selectivity (♦) was calculated by dividing the signal measured in solution with chlorine (○) by the absolute value of the signal measured in solution without chlorine (□).

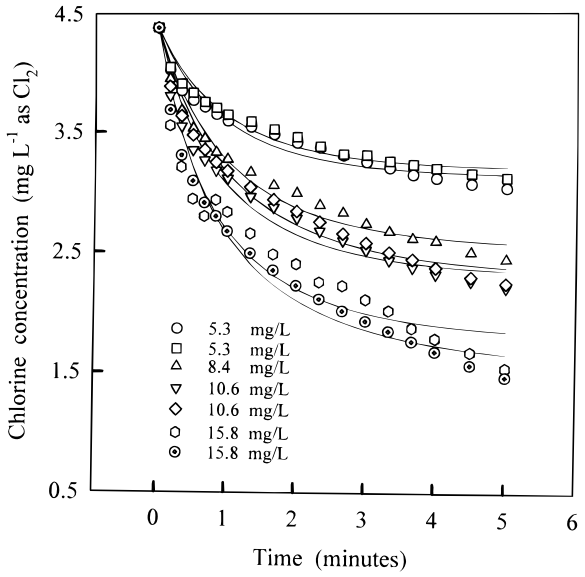

FIGURE 3. Typical kinetic data for batch reaction of chlorine with suspended cell biomass. The data are for various initial biomass concentrations. Lines are regression results fitting eqs 3 and 4 to individual data sets.

Chlorine reacted with cell mass and with agarose. Kinetic rate coefficients were determined by analysis of chlorine concentration versus time data collected in suspended biomass batch reaction experiments; an example is reproduced in Figure 3. The kinetic form of the model we used, which assumed first-order dependence of the reaction rate on chlorine and biomass concentrations, adequately captured the observed behavior. Chlorine reacted much more rapidly with cellular biomass than it did with agarose. The chlorine−biomass reaction rate coefficient averaged $1.1 \times 10^{-3} \pm 0.3 \times 10^{-3}$ L mg^{-1} s^{-1} in short-duration experiments (Table 2) and $4.7 \times 10^{-4} \pm 1.0 \times 10^{-4}$ L mg^{-1} s^{-1} in long-duration experiments (Table 3). The chlorine−agarose reaction rate coefficient was ap-

TABLE 2

Chlorine−Cell Reaction Rate and Yield Coefficients from Short-Duration Experiments[a]

C_o (mg L^{-1})	X_{1o} (mg L^{-1})	k_1 (L mg^{-1} s^{-1})	Y_1 (mg/mg)
4.2	4.62	8.3×10^{-4}	3.1
4.2	4.62	12.5×10^{-4}	3.2
4.2	9.24	13.5×10^{-4}	3.6
4.2	9.24	14.2×10^{-4}	3.2
4.2	23.1	15.2×10^{-4}	6.2
4.2	23.1	15.8×10^{-4}	6.4
4.38	5.28	10.3×10^{-4}	4.2
4.38	5.28	9.5×10^{-4}	4.4
4.38	8.44	9.2×10^{-4}	4.6
4.38	10.6	9.3×10^{-4}	5.1
4.38	10.6	8.0×10^{-4}	5.1
4.38	15.8	8.8×10^{-4}	6.1
4.38	15.8	8.5×10^{-4}	5.6
4.68	6.94	9.3×10^{-4}	3.7
4.68	6.94	13.8×10^{-4}	4.1
4.68	10.4	11.2×10^{-4}	5.1
4.68	10.4	11.2×10^{-4}	4.4
4.68	13.9	14.7×10^{-4}	4.0
4.68	13.9	17.5×10^{-4}	4.5
7.96	2.2	9.5×10^{-4}	3.1
7.96	5.5	9.8×10^{-4}	3.6
7.96	5.5	10.2×10^{-4}	3.5
7.96	8.25	8.5×10^{-4}	3.9
7.96	8.25	7.2×10^{-4}	3.7
7.96	11.0	9.8×10^{-4}	3.2
	av	11.2×10^{-4}	4.3
	SD	2.7×10^{-4}	1.0

[a] The parameters are C_o, initial chlorine concentration; X_{1o}, initial biomass concentration; k_1, biomass−chlorine reaction rate coefficient; Y_1, biomass−chlorine yield coefficient.

TABLE 3

Chlorine−Cell Reaction Rate and Yield Coefficients from Long-Duration Experiments[a]

C_o (mg L^{-1})	X_{1o} (mg L^{-1})	k_1 (L mg^{-1} s^{-1})	Y_1 (mg mg^{-1})
7.01	1.80	5.3×10^{-4}	0.61
7.11	1.80	4.5×10^{-4}	0.29
7.01	2.66	3.0×10^{-4}	0.72
7.01	2.88	4.3×10^{-4}	0.57
7.01	3.50	6.5×10^{-4}	0.59
7.01	5.31	4.5×10^{-4}	0.75
	av	4.7×10^{-4}	0.59
	SD	1.0×10^{-4}	0.15

[a] The parameters are C_o, initial chlorine concentration; X_{1o}, initial biomass concentration; k_1, biomass−chlorine reaction rate coefficient; Y_1, biomass−chlorine yield coefficient.

proximately 2 orders of magnitude smaller, averaging 3.7 $\times 10^{-6}$ L mg^{-1} s^{-1} (Table 4). Yield coefficients determined in these batch suspended biomass experiments ranged from 0.60 to 4.3 mg of cell biomass/mg of Cl to 540 mg of agarose/mg of Cl (Tables 2−4).

The rate of chlorine penetration into artificial biofilms, as directly measured with a microelectrode, depended on the biofilm cell density and biofilm thickness. Chlorine penetrated a pure agarose film containing no cells (773 μm thick) within 10−15 min (Figure 4A). Penetration was retarded when cells were incorporated into the gel matrix, even when the biofilm was thinner (Figure 4B, 428 μm thick biofilm). In one experiment in which a 526 μm thick film containing 14 400 mg of cell mass/L initially was treated with 18.6 mg L^{-1} chlorine, the concentration of chlorine at the substratum only rose to 1.8 mg L^{-1} after 3 h of exposure to the chlorine solution. Chlorine concentration profiles were measured in a total of six experiments with different initial biomass densities and biofilm thicknesses.

TABLE 4

Chlorine−Agarose Reaction Rate and Yield Coefficients[a]

C_o (mg L^{-1})	X_{2o} (mg L^{-1})	k_2 (L mg^{-1} s^{-1})	Y_2 (mg mg^{-1})
1.13	200	3.7×10^{-6}	490
2.25	200	4.1×10^{-6}	590
3.00	200	3.3×10^{-6}	540
	av	3.7×10^{-6}	540
	SD	0.3×10^{-6}	42

[a] The parameters are C_o, initial chlorine concentration; X_{2o}, initial agarose concentration; k_2, agarose−chlorine reaction rate coefficient; Y_2, agarose−chlorine yield coefficient.

Two control experiments were also performed to assess the influence of the substratum and of the artificial biofilm matrix on electrode response. The chlorine profile in the flowing fluid adjacent to a clean substratum (no artificial biofilm of any kind) was flat, indicating that the substratum itself did not perturb chlorine measurement by the microelectrode. A flat response was also recorded when the electrode penetrated an artificial biofilm in a chlorine-free solution; this showed that the agarose−cell gel did not induce any artifactual signal.

Transient penetration of chlorine into artificial biofilm was calculated using an unsteady reaction−diffusion model, and the theoretical simulations were compared to experimentally measured chlorine concentration profiles. Parameter values were either experimentally determined or estimated from correlations (Table 5). As explained below, one parameter value, Y_1, was adjusted to obtain the match to experimental data presented in Figure 4.

In previous work (*7*, *19*), we have used a literature value (*10*) for the diffusion coefficient of chlorine in water of 1.44 $\times 10^{-5}$ cm^2 s^{-1}. This value, however, appears to correspond to diatomic chlorine. At the pH of our experiments, the chlorine species in solution are hypochlorous acid and hypochlorite ion. The Wilke−Chang correlation was used, therefore, to estimate the diffusion coefficient of HClO with the resulting value of 2.67 $\times 10^{-5}$ cm^2 s^{-1} (*10*). The ratio of the effective diffusion coefficient in the biofilm to the diffusion coefficient in water was estimated from a correlation suggested by Westrin and Axelsson (*11*) that accounts for reduction in effective diffusion coefficient due to the polymer content of the film. The cell volume fraction in artificial biofilms was always less than 0.1% and so was expected to have a negligible effect on diffusion coefficients.

Theoretical and empirical correlations for the external mass transfer coefficient were used to estimate the dimension of a fictitious stagnant liquid film, δ. With a Reynolds number (based on mean hydraulic radius) of 660 in the flow cell system, δ was calculated to be 148 μm and 98 μm, respectively, for the two approaches used (*12*, *13*). A value of 100 μm was used in model simulations; this value is also close to the values estimated by inspection of experimental chlorine profiles.

In preliminary model runs, it was observed that the time course of chlorine penetration was particularly sensitive to the yield coefficient relating the proportions in which

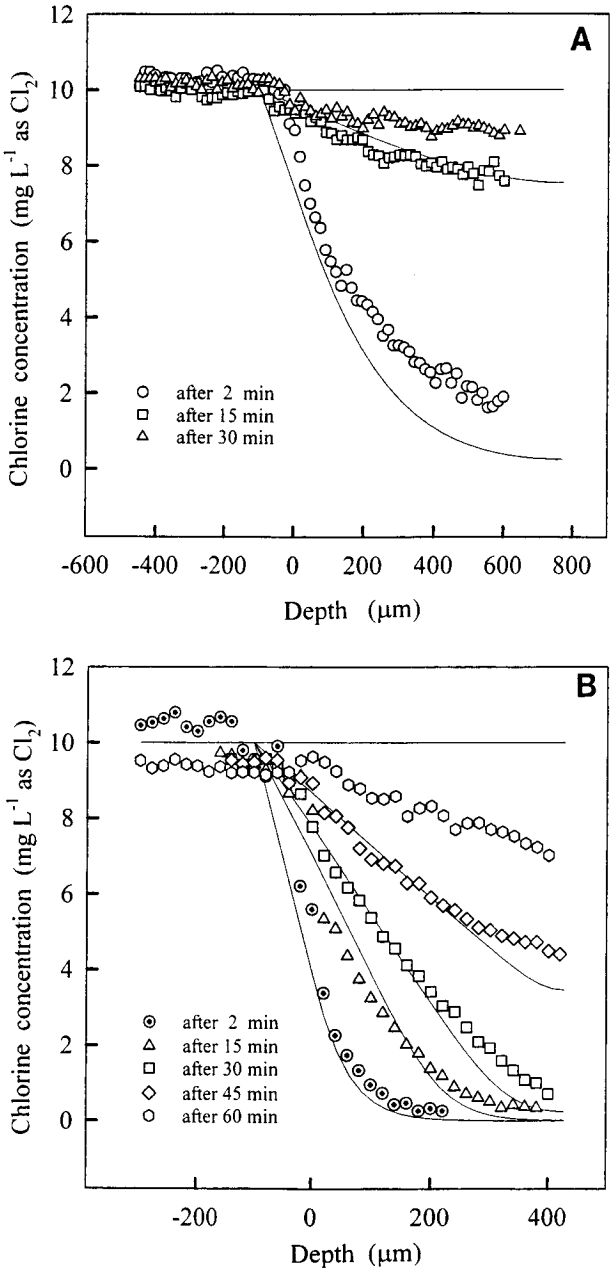

FIGURE 4. Transient chlorine concentration profiles in artificial biofilms. Negative numbers on the *x*-axis represent the bulk fluid, and zero corresponds to the interface between the bulk fluid and biofilm. Sequential data sets collected at different times after the onset of chlorine treatment are shown. Panel A corresponds to a 773 μm thick film containing agarose but no cells. Panel B corresponds to a 428 μm thick film containing both cells and agarose.

biomass and chlorine are consumed, Y_1. The experimentally determined range of this yield coefficient was also broad, with estimates from short-duration and long-duration experiments differing by a factor of 7. To obtain an adequate match between model simulations and experimental data, the value of Y_1 was adjusted. The fit between experiment and theory was judged by visual inspection. Values of Y_1 that fit the data well were consistently near 1.8 mg mg^{-1}, which is midway between the values determined experimentally. In short-duration experiments (5 min), Y_1 averaged 4.3 mg mg^{-1}, whereas in long-duration experiments (20 h) Y_1 averaged 0.6 mg mg^{-1}. The duration of most of the chlorine concentration profile experiments was 2 h.

The time required for chlorine to penetrate biofilm was also expressed in dimensionless form by dividing the experimentally determined time required to attain 50% of the bulk solution concentration at the substratum by the theoretically predicted time for a nonreactive tracer to reach the same degree of penetration in a biofilm of the same dimension:

$$\tau_{50} = \frac{t_{50} D_e}{0.379 L_f^2} \tag{11}$$

where t_{50} is the experimentally measured penetration time in seconds. If there were no interaction of the penetrating molecule with the biofilm, τ_{50} would be 1. The extent by which τ_{50} exceeds 1 is a measure of the retardation of biocide penetration. In an earlier theoretical study (*14*), it was predicted that τ_{50} is essentially directly proportional to the "reactive capacity" of the biofilm, denoted by ρ, where

$$\rho = \frac{X_1/Y_1 + X_2/Y_2}{C_o} \tag{12}$$

As shown in Figure 5, τ_{50} ranged from close to 1 to greater than 100 and was approximately directly proportional to ρ. In physical terms, this means that the degree of retardation of chlorine penetration is directly proportional to the biomass density of the biofilm and inversely proportional to the bulk chlorine concentration.

Discussion

Chlorine reacted rapidly with cellular biomass and also reacted, though much more slowly, with agarose. The order of magnitude of the reaction rate between chlorine and microbial biomass was comparable to that reported in earlier studies (*15*−*17*). The rate of reaction was sufficient to account for the failure of chlorine to penetrate artificial biofilms during treatment with chlorine solutions (10−20 mg L^{-1}) over periods of several hours. More specifically, the penetration failure can be attributed to a reaction−diffusion interaction in which chlorine is neutralized by reaction with biofilm constituents faster than it diffuses into the biofilm. Related evidence for such a mechanism of reduced biofilm susceptibility includes chlorine concentration profiles measured in a natural biofilm (*7*), spatial gradients in physiological activity within biofilms in response to disinfection by monochloramine (*18*), chlorine penetration and disinfection efficacy of bacteria entrapped in alginate gel beads (*19*), calculation of monochloramine flux into biofilm (*20*), and biocide reaction rate measurements (*21*).

The penetration time of chlorine into biofilm is proportional to the biofilm cell density. Our experiments were conducted at cell densities substantially lower than those encountered in real biofilms. Extrapolating our results to natural biofilms, for example, with an assumed biomass density of 20 000 mg L^{-1} and thickness of 500 μm, the time required to reach 50% of the bulk fluid chlorine concentration at the substratum for a 2 mg L^{-1} chlorine treatment would be 114 h. The analogous penetration time for a nonreactive tracer in the same biofilm would be approximately 44 s. In experiments with bacteria entrapped in 3 mm diameter alginate gel beads, chlorine penetration times on the order of days were determined (*19*). The retardation of chlorine penetration in real biofilm systems, therefore, may be profound.

TABLE 5

Parameter Input Values for Biofilm Modeling[a]

parameter	symbol	case A	case B
initial cell mass concn (mg L^{-1})	X_{1o}	0	901
initial agarose concn (mg L^{-1})	X_{2o}	20 000	10 000
biofilm thickness (μm)	L_f	773	428
concn boundary layer thickness (μm)	δ	100	100
bulk fluid chlorine concn (mg L^{-1})	C_o	10.4	9.8
chlorine effective diffusion coeff ($cm^2\ s^{-1}$)	D_e	2.4×10^{-5}	2.5×10^{-5}
chlorine−cell reaction rate coeff (L $mg^{-1}\ s^{-1}$)	k_1	0.0	1.1×10^{-3}
chlorine−agarose reaction rate coeff (L $mg^{-1}\ s^{-1}$)	k_2	3.7×10^{-6}	3.7×10^{-6}
cell−chlorine yield coeff (mg mg^{-1})	Y_1	0.0	1.85
agarose−chlorine yield coeff (mg mg^{-1})	Y_2	540	540

[a] Case A corresponds to Figure 4A, and case B corresponds to Figure 4B.

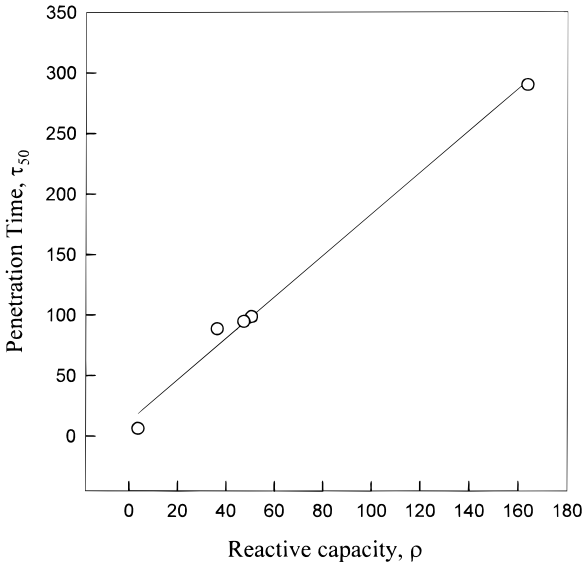

FIGURE 5. Dimensionless chlorine penetration time as a function of biofilm reactive capacity. The line is the least squares regression given by $\tau_{50} = 1.72\rho + 12.3$ ($r^2 = 0.992$).

The magnitude of the biomass−chlorine yield coefficient, Y_1, which was measured to be in the range of 0.6−4.3 mg of biomass/mg of chlorine, indicates only partial oxidation of biomass by chlorine. Assuming $C_5H_7O_2N$ as a representative biomass composition, complete oxidation to carbon dioxide, water, and nitrogen gas would result in a yield coefficient of 0.27 mg mg^{-1}. Thus, reactions between biomass constituents and chlorine may result in depletion of chlorine reactive sites in the biomass without entirely destroying or consuming the biomass.

This study reinforces the potential utility of a biofilm model that incorporates biocide transport and reaction for optimizing biocide applications. Such a model, of which there are preliminary versions (*14*, *22*, *23*), could be used to design biocide delivery protocols that maximize biocide efficacy while minimizing environmental impact. Some aspects of the model require refinement. For example, it is clear from the measurements of yield coefficient reported in this paper that there are likely to be multiple reactions between chlorine and biomass constituents. Parallel reactions could explain why the yield coefficient, Y_1, and reaction rate coefficient, k_1, varied between short-term and long-term experiments. It may be necessary to distinguish parallel reactions with different kinetic and stoichiometric coefficients to obtain a truly predictive model.

Acknowledgments

This work was supported through Cooperative Agreement EEC-8907039 between the National Science Foundation and Montana State University and by the industrial partners of the Center.

Literature Cited

(1) Costerton, J. W.; Cheng, K. J.; Geesey, G. G.; Ladd, T. I.; Nickel, J. C.; Dasgupta, M.; Marrie, T. J. *Annu. Rev. Microbiol.* **1987**, *41*, 435−464.
(2) LeChevallier, M. W.; Cawthon, C. D.; Lee, R. G. *Appl. Environ. Microbiol.* **1988**, *54*, 2492−2499.
(3) Nichols, W. W. *Structure and Function of Biofilms*; Characklis, W. G.; Wilderer, P. A., Eds.; John Wiley & Sons Inc.: New York, 1989; pp 321−331.
(4) Amato, I. *Science* **1993**, *261*, 152−154.
(5) Puckorius, P. *Power* **1994**, *138*, 57−58.
(6) McCoy, J. W. *Microbiology of Cooling Water*; Chemical Publishing Co.: New York, 1980.
(7) de Beer, D.; Srinivasan, R.; Stewart, P. S. *Appl. Environ. Microbiol.* **1994**, *60*, 4339−4344.
(8) Bakke, R.; Olsson, P. Q. *J. Microbiol. Methods* **1986**, *5*, 93−98.
(9) *Standard Methods for the Examination of Water and Wastewater*, 18th ed.; American Public Health Association: Washington, DC, 1992; pp 4-43−4-48.
(10) Perry, R. H.; Green, D. W.; Maloney, J. O. *Perry's Chemical Engineers' Handbook*, 6th ed.; McGraw-Hill: New York, 1984; pp 3−286.
(11) Westrin, B. A.; Axelsson, A. *Biotechnol. Bioeng.* **1991**, *38*, 439−446.
(12) Bennett, C. O.; Myers, J. E. *Momentum, Heat, and Mass Transfer*, 2nd ed.; McGraw-Hill: New York, 1974; p 540.
(13) Geankolis, C. J. *Transport Processes and Unit Operations*, 2nd ed.; Allyn and Bacon Inc: Newton, MA, 1983; p 433.
(14) Stewart, P. S.; Raquepas, J. B. *Chem. Eng. Sci.* **1995**, *50*, 3099−3104.
(15) Characklis, W. G.; Dydek, S. T. *Water. Res.* **1975**, *10*, 515−522.
(16) van der Wende, E. Ph.D. Dissertation, Montana State University, Bozeman, MT, 1991.
(17) Characklis, W. G.; Trulear, M. G.; Stathopoulos, N. R. *Water Chlorination: Environmental Impact and Health Effects*; Jolley, L., Brungs, W. A., Cumming, R. B., Jacobs, V. A., Eds.; Ann Arbor Science: Ann Arbor, MI, 1980; pp 349−368.
(18) Huang, C.-T., Yu, F. P., McFeters, G. A., Stewart, P. S. *Appl. Environ. Microbiol.* **1995**, *61*, 2252−2256.
(19) Xu, X.; Stewart, P. S.; Chen, X. *Biotechnol. Bioeng.* **1996**, *49*, 93−100.
(20) Chen, C.; Griebe, T.; Characklis, W. G. *Biofouling* **1993**, *7*, 1−17.
(21) Tashiro, H.; Numakura, T.; Nishikawa, S.; Miyaji, Y. *Water Sci. Technol.* **1991**, *23*, 1395−1403.
(22) Stewart, P. S. *Antimicrob. Agents Chemother.* **1994**, *38*, 1052−1058.
(23) Stewart, P. S.; Hamilton, M. A.; Goldstein, B. R.; Schneider, B. T. *Biotechnol. Bioeng.* **1996**, *49*, 445−455.

Received for review December 6, 1995. Revised manuscript received February 1, 1996. Accepted February 1, 1996.[⊗]

ES9509184

[⊗] Abstract published in *Advance ACS Abstracts,* April 1, 1996.